

Electronic Supplementary Information

The effect of silica on polymorphic precipitation of calcium carbonate: an on-line energy-dispersive X-ray diffraction (EDXRD) study

Matthias Kellermeier,^a, Fabian Glaab,^b Regina Klein,^b Emilio Melero-García,^c
Werner Kunz,^b and Juan Manuel García-Ruiz*^c*

^a Physical Chemistry, University of Konstanz, Universitätsstrasse 10,
D-78457 Konstanz, Germany

^b Institute of Physical and Theoretical Chemistry, University of Regensburg,
Universitätsstrasse 31, D-93040 Regensburg, Germany

^c Laboratorio de Estudios Cristalográficos, IACT (CSIC-UGR), Avda. del Conocimiento s/n,
P.T. Ciencias de la Salud, E-18100 Armilla, Spain

Section S1: Additional Figures and Tables

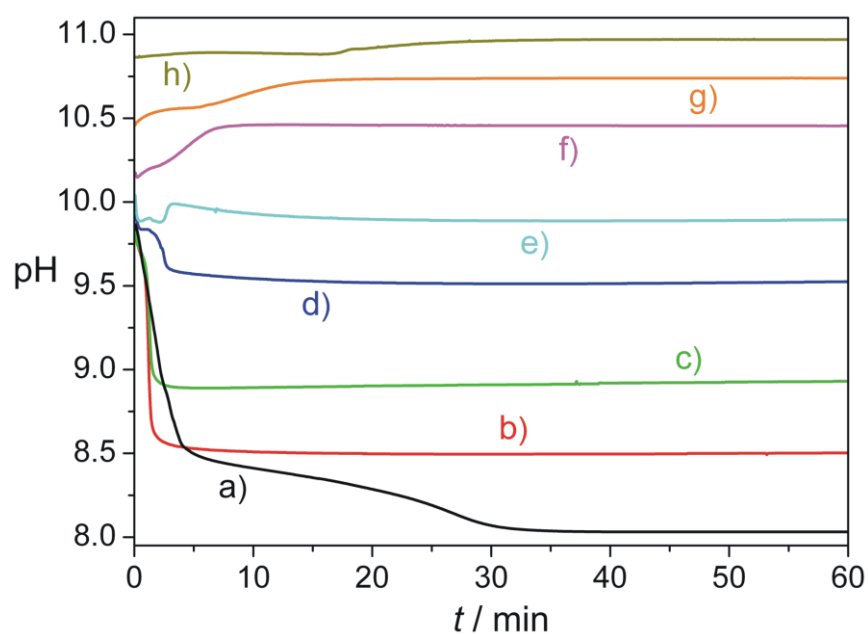


Fig. S1. Temporal evolution of the pH during crystallisation of calcium carbonate from solutions at 20°C and $[\text{Ca}^{2+}] = [\text{CO}_3^{2-}] = 250$ mM in the presence of (a) 0, (b) 200, (c) 600, (d) 1200, (e) 2000, (f) 5000, (g) 10000, and (h) 20000 ppm SiO_2 , monitored over a period of 60 min after mixing reagents.

[SiO₂] / ppm (before mixing)		pH	
<i>expected</i>	<i>measured</i>	<i>before mixing</i>	<i>after mixing (40 min)</i>
0	0	11.68	8.39
400	392	11.65	8.50
1200	1101	11.57	8.92
2400	2348	11.56	9.51
4000	3824	11.50	9.89
10000	9967	11.47	10.46
20000	19372	11.54	10.74
40000	41613	11.66	10.97

Table S1. Silica concentration and pH of 0.5 M Na₂CO₃ solutions before (and after) mixing with 0.5 M CaCl₂ (final SiO₂ contents in the samples thus being half of the values shown here). The amount of dissolved silica was measured by means of the molybdate yellow method according to a procedure described elsewhere,^{S1} giving concentrations of “reactive silica” (essentially mono- and dimers) that agree with expected values within the limits of experimental error. Note that purging of the silica/carbonate mixtures with N₂ over several hours (to drive out CO₂) did not lead to any significant change in the measured SiO₂ concentration, as all solutions are undersaturated with respect to amorphous silica at pH levels ≥ 11.5 (i.e. prior to mixing with CaCl₂).^{S2} While the pH is roughly independent of the silica content and dominated by the carbonate alkalinity before addition of Ca²⁺, it increases continuously with the SiO₂ concentration after CaCO₃ precipitation due to the basic character of the additive (see also Section S2).

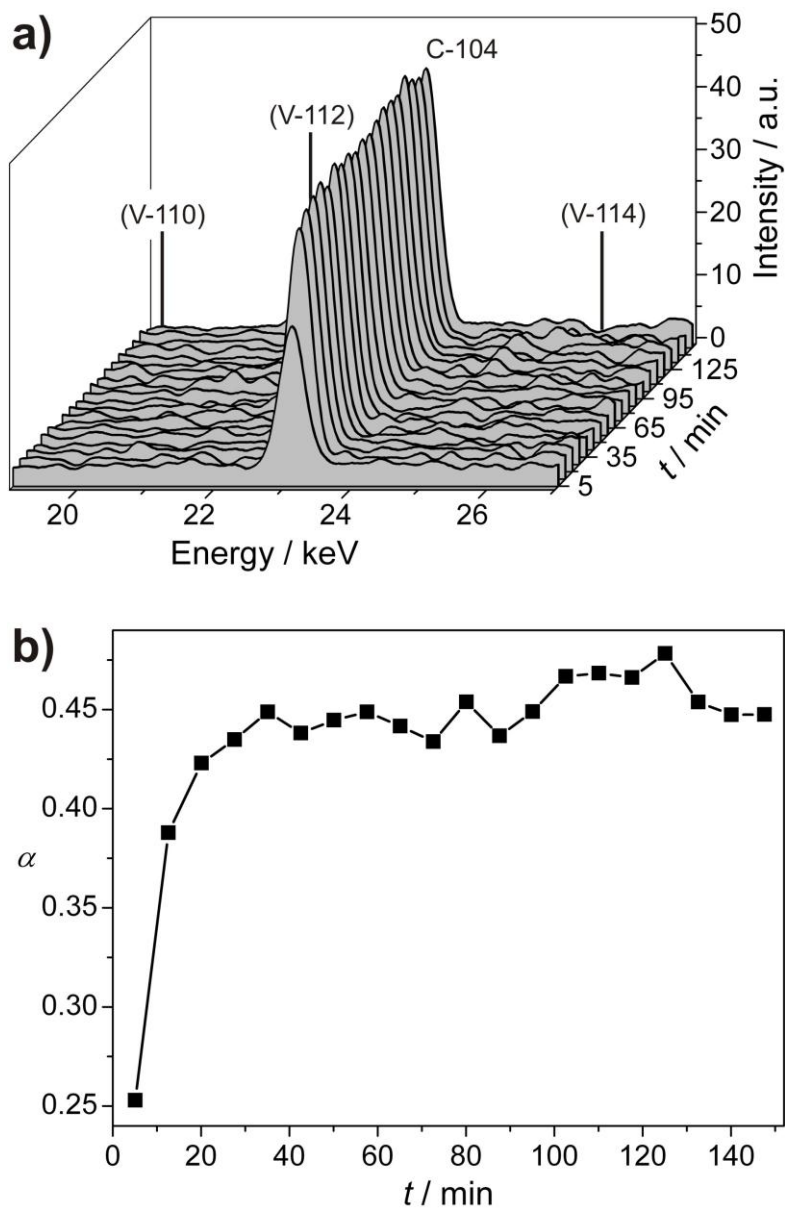


Fig. S2. Temporal evolution of (a) the calcite 104 reflection in diffraction patterns and (b) the calculated reaction progress α for a sample containing 10000 ppm SiO_2 at 50°C . The interval of energies shown in (a) is chosen such that the region where the strongest vaterite peaks (indicated by vertical lines and their Miller indices) would be expected is also covered.

Section S2: Experimental Details and Data Evaluation

S2.1 Materials and Methods

The following chemicals were used as received: calcium chloride dihydrate (Riedel-de Haën, ACS reagent, $\geq 99\%$), sodium carbonate (Roth, anhydrous, $\geq 99\%$), sodium silicate solution (“water glass”, Sigma-Aldrich, reagent grade, containing 26.7 wt% SiO_2). All solutions were prepared using water of Milli-Q quality. Dilute silica sols were bubbled with H_2O -saturated N_2 for several hours in order to remove CO_2 ingested by the water glass stock during storage, and then used to dissolve Na_2CO_3 . The resulting silica/carbonate mixtures were filtered (450 nm) and subsequently kept in tightly stoppered plastic bottles under a N_2 atmosphere until shortly before measurement, so as to avoid both uptake of CO_2 from the air and leaching out of additional silica from glass walls.

Precipitation was carried out in cylindrical quartz vials (Duran, culture tubes, outer dimensions: 12x100 mm), which had previously been cleaned by successive treatment with a solution of KOH in isopropanol, 3 M HCl, and boiling 30% HNO_3 , followed by extensive rinsing with water and drying at 120°C . Immediately after mixing reagents, the quartz tubes containing the samples were inserted into a custom-designed glass jacket which was centred in the beam and had windows on both sides of the vial, allowing the X-rays to pass the solutions without the need to travel through the outer mantle. A sketch depicting the assembly used for the experiments is shown in Fig. S3. The glass jacket surrounding the tubes was circulated by oil supplied from a thermostat (Julabo FP50), which was regulated such that the temperature of the solution inside the tubes was kept constant at 20, 50 and 80°C , respectively. The temperature accuracy of the setup is estimated to $\pm 0.5^\circ\text{C}$. During data collection, solutions were stirred at a constant frequency of 1200 rpm by a magnetic plate placed underneath the thermostatted jacket, ensuring that precipitated material was evenly suspended and thus uniformly hit by the beam.

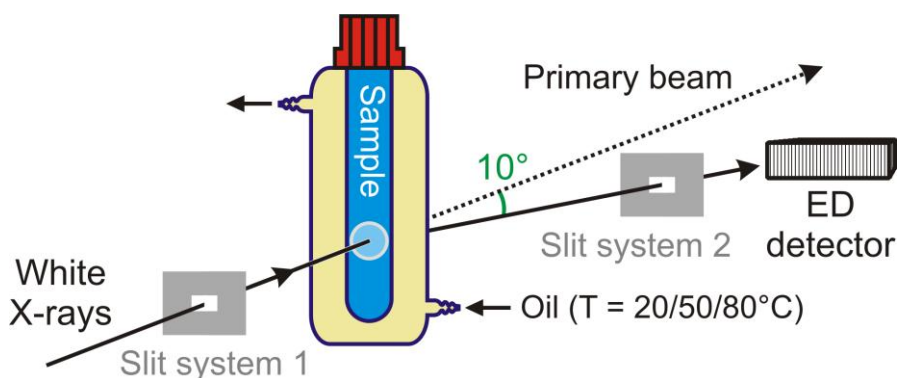


Fig. S3 Scheme of the experimental setup used for EDXRD measurements.

S2.2 Data Processing and Evaluation

The obtained raw data were first normalised for the time-dependent intensity of the incident beam, that is, spectra were divided by the mean ring current operating during the respective run. Subsequently and before any further processing of the data, the integral area of the most important reflections was determined relative to the background for each of the polymorphs occurring in the respective sample, which were 104 ($E_{C-104} \approx 23.1$ keV, $d_{Lit} = 3.035$ Å) for calcite, 110 ($E_{V-110} \approx 19.7$ keV, $d_{Lit} = 3.573$ Å), 112 ($E_{V-112} \approx 21.3$ keV, $d_{Lit} = 3.294$ Å) and 114 ($E_{V-114} \approx 25.7$ keV, $d_{Lit} = 2.730$ Å) for vaterite, and 111 ($E_{A-111} \approx 21.4$ keV, $d_{Lit} = 4.341$ Å) as well as 021 ($E_{A-021} \approx 25.9$ keV, $d_{Lit} = 2.734$ Å) for aragonite.^{S3} Based on the results and since the only phase detected at the end of experiments conducted in the absence of silica was calcite, the reaction progress α as a function of time was defined and calculated as the ratio of the integral area for the calcite 104 reflection of the sample at time t and the corresponding average value determined for the silica-free reference at each temperature after complete conversion to calcite, according to:

$$\alpha(t) = \frac{A_{C-104}(t)}{A_{C-104, final}} \quad (\text{Equation S1})$$

The relative fraction of calcite (f_C) present at a given time in binary mixtures with vaterite, typically encountered at 20 and 50°C, was derived using Rao's equation but employing integrated peak areas instead of maximum intensities:^{S4}

$$f_C = \frac{A_{C-104}}{A_{C-104} + A_{V-110} + A_{V-112} + A_{V-114}} \quad (\text{Equation S2})$$

For systems in which calcite coexisted with aragonite, as commonly observed at 80°C, f_C was obtained from the peak areas of the two nominally strongest reflections, i.e. calcite-104 and aragonite-111, utilising an empirical relation suggested by Wada et al. (Equation S3).^{S5}

$$f_C = \frac{1}{1 + 3.9 \cdot A_{A-111}/A_{C-104}} \quad (\text{Equation S3})$$

Since none of the samples contained all three polymorphs, the fraction of the occurring metastable phase could readily be calculated via $f_{V/A} = 1 - f_C$. Note that values for α and f as well as diffraction patterns are referred to the time when half of the corresponding measurement run was completed.

After the above evaluations, data were further processed to facilitate graphical visualisation of the temporal evolution in the diffraction patterns. First, background scattering originating mainly from the glass walls of the vials and water was subtracted by fitting 50-point baselines to the broad amorphous hillock extending over almost the entire raw spectra. Background-corrected patterns were subsequently smoothed using a moving-average routine with a box width of 10 points, in order to reduce noise. This procedure did not affect peak heights and areas to a noticeable extent. Finally, to enable a better comparison, intensity values of patterns acquired for samples with various silica concentrations at a given temperature were normalised with respect to the final peak maximum of the calcite 104 reflection in the corresponding reference without added silica, which was arbitrarily set to $I = 100$. With the processed data, two-dimensional (2D) intensity contour plots as well as three-dimensional

(3D) representations of time-dependent pattern series were generated. Selected graphs are shown in the main text, while the full dataset is reproduced below (Section S3).

Section S2: pH Measurements

Since the pH is a crucial parameter for the chemistry of both carbonate and silicate in aqueous media and, thus, provides information on their speciation in solution as well as on-going precipitation (or polymerisation) processes, it was measured exemplarily at 20°C for samples at different silica concentrations in an independent series of experiments. To that end, reagents were combined in small beakers, and a glass electrode (Mettler-Toledo InLab Micro) was quickly immersed in the solution. The system was sealed against the atmosphere using Parafilm and the pH was measured under vigorous stirring with a Schott laboratory pH meter (model CG-843) connected to a computer. Values were read continuously in steps of 5 s over a total period of 60 min after mixing. The resulting time-dependent progressions for the first hour after combining reagents are shown in Fig. S1.

When no silica is added (Fig. S1a), the pH – initially being about 9.8-9.9 – drops to values below 8.5 within the first 5 min after mixing, which reflects the precipitation of CaCO_3 from solution and has been described as “unstable stage” or induction period in the literature.^{S6,S7} During this interval, ACC particles are likely to be generated. Their transformation to crystalline polymorphs is accompanied by a decrease in pH due to the higher solubility of ACC relative to the anhydrous phases,^{S8} which causes the concentration of carbonate ions (and hence the alkalinity) to lower in the course of transformation. ACC conversion is essentially completed once the initial steep decline in pH is terminated (i.e. after ~5 min). At this point, a plateau is reached and the pH decays only slightly in the following before, at around 25 min, a second step-like decrease from about 8.3 to 8.0 is observed, subsequent to which there are no further significant changes in pH with time. The occurrence of a plateau in the pH-time curve and the found two-step decrease suggest that a metastable crystalline

polymorph, likely vaterite at the given temperature, was formed as an intermediate phase and fully converted to calcite after a certain delay.^{S7} Because calcite is less soluble than vaterite^{S8} and the concentration of dissolved carbonate ions is determined by the solubility product of the most soluble phase, the pH will correspond to the value set by vaterite as long as it occurs in noticeable amounts in the samples. Thus, the pH data hint at a significant fraction of vaterite being generated during the early stages of precipitation in the absence of silica at 20°C, which is consistent with the results of EDXRD measurements (cf. main text). Moreover, the apparent period for which the metastable intermediate persists in solution before being completely transformed to calcite (25-30 min as judged from the pH curve) is in fair agreement with what is estimated for the lifetime of vaterite on the basis of the diffraction patterns (30-40 min, cf. Fig. 3a in the main text).

On addition of silica, the initial pH of the mixtures does at first not change markedly. Only at concentrations equal to or higher than 5000 ppm SiO₂, the basic character of the additive becomes noticeable and gradually increases the starting pH to values between 10 and 11 (Fig. S1f-h). Precipitation of CaCO₃ at silica contents of 200-1200 ppm leads to an instant decrease in pH as observed for the silica-free reference (Fig. S2b-d). However, the final pH of the samples is the higher the more silica was added and, importantly, the pH remains constant immediately after the induction period has expired. These findings can be explained by the buffering ability of silica, which maintains the pH at the level corresponding to the particular concentration once the major part of the carbonate ions has precipitated. This implies that conclusions on possibly occurring metastable intermediate phases and crystallization kinetics can no longer be drawn from the pH data when silica is present.

It is interesting to note that, for silica contents of 2000-10000 ppm, the initial decrease in pH observed for lower concentrations turns into an increase with time (cf. Fig. S1e-g). Presumably, this feature originates from enhanced silica condensation reactions, which consume acidic silanol groups and hence raise the pH.^{S9} This suggests that samples at higher

silica contents contain an appreciable amount of polymerised silicates (which may readily adsorb on or co-precipitate with CaCO₃ polymorphs). Oligomerisation of silica might be triggered by the presence of free Ca²⁺ ions which screen negative charges and thereby facilitate condensation.^{S10} Alternatively, the formation of CaCO₃ could by itself induce polymerisation of siliceous species due to local changes in conditions around carbonate particles growing in alkaline media, as demonstrated previously for ACC.^{S2} Moreover, the period over which silica condensation is active increases with its concentration, from ~3 min at 2000 ppm SiO₂ to around 15 min at 10000 ppm. This suggests that, either, condensation is slower at higher concentrations or, more probably, a growing fraction of silica polymerises. At a SiO₂ content of 20000 ppm, there are in turn hardly any changes of pH with time (Fig. S2h), likely due to the large excess of silica which effectively buffers any on-going processes.

References

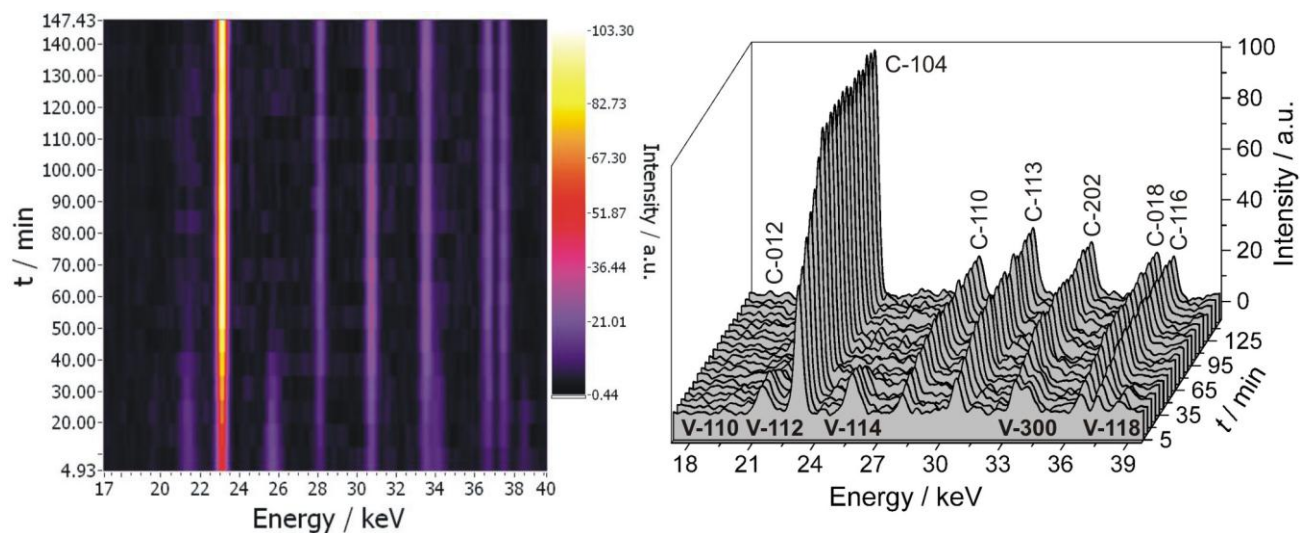
- [S1] M. Kellermeier, E. Melero-Garcia, F. Glaab, J. Eiblmeier, L. Kienle, R. Rachel, W. Kunz and J. M. Garcia-Ruiz, *Chem. Eur. J.*, 2012, **18**, 2272.
- [S2] M. Kellermeier, E. Melero-Garcia, F. Glaab, R. Klein, M. Drechsler, R. Rachel, J. M. Garcia-Ruiz and W. Kunz, *J. Am. Chem. Soc.*, 2010, **132**, 17859.
- [S3] JCPDS Cards No. 5-586 (calcite), 33-268 (vaterite), and 71-2392 (aragonite).
- [S4] M. S. Rao, *Bull. Chem. Soc. Jpn.*, 1973, **46**, 1414.
- [S5] N. Wada, M. Okazaki and S. Tachikawa, *J. Cryst. Growth*, 1993, **132**, 115.
- [S6] T. Ogino, T. Suzuki and K. Sawada, *Geochim. Cosmochim. Acta*, 1987, **51**, 2757.
- [S7] D. Kralj, L. Brecevic and J. Kontrec, *J. J. Cryst. Growth*, 1997, **177**, 248.
- [S8] L. Brecevic and A. E. Nielsen, *J. Cryst. Growth*, 1989, **89**, 504.
- [S9] A. E. Voinescu, M. Kellermeier, A. M. Carnerup, A. K. Larsson, D. Touraud, S. T. Hyde and W. Kunz, *J. Cryst. Growth*, 2007, **306**, 152.
- [S10] R. K. Iler, *The chemistry of silica*, Wiley, New York, 1979.

Section S4: Full EDXRD dataset

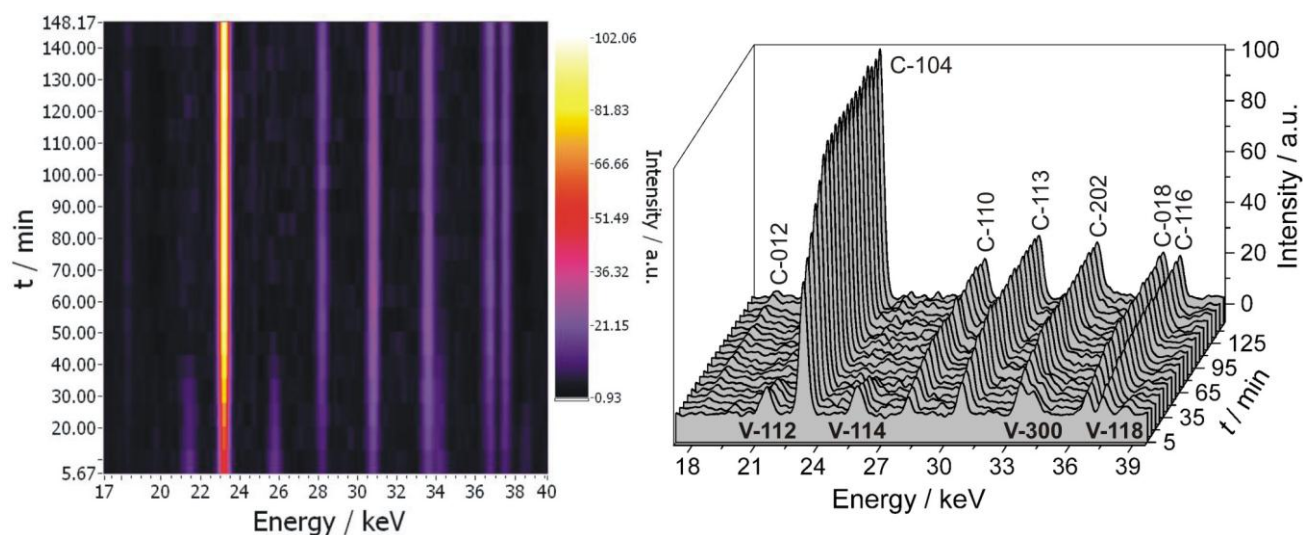
In the following, the full set of EDXRD data discussed in this work is reproduced. Successively, time-dependent diffraction patterns of samples with increasing silica content are illustrated for reaction temperatures of 20, 50 and 80°C in the form of 2-D contour plots (left) as well as by means of 3-D representations (right), in which the occurring reflections are assigned to families of planes in the calcite (C), vaterite (V), or aragonite (A) lattice.

20°C

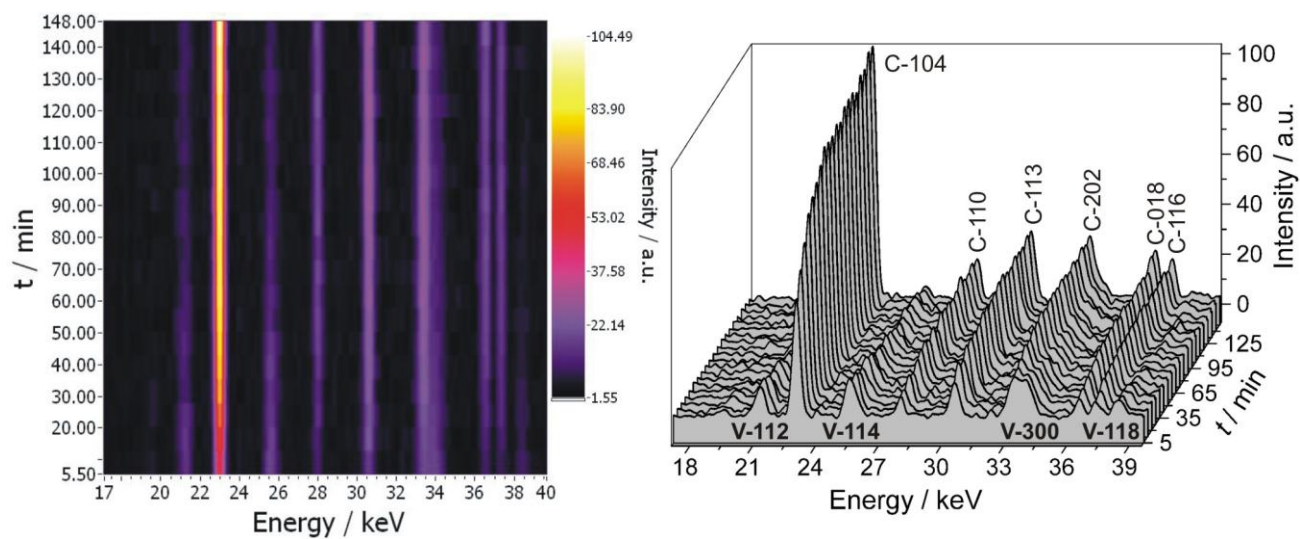
0 ppm SiO₂



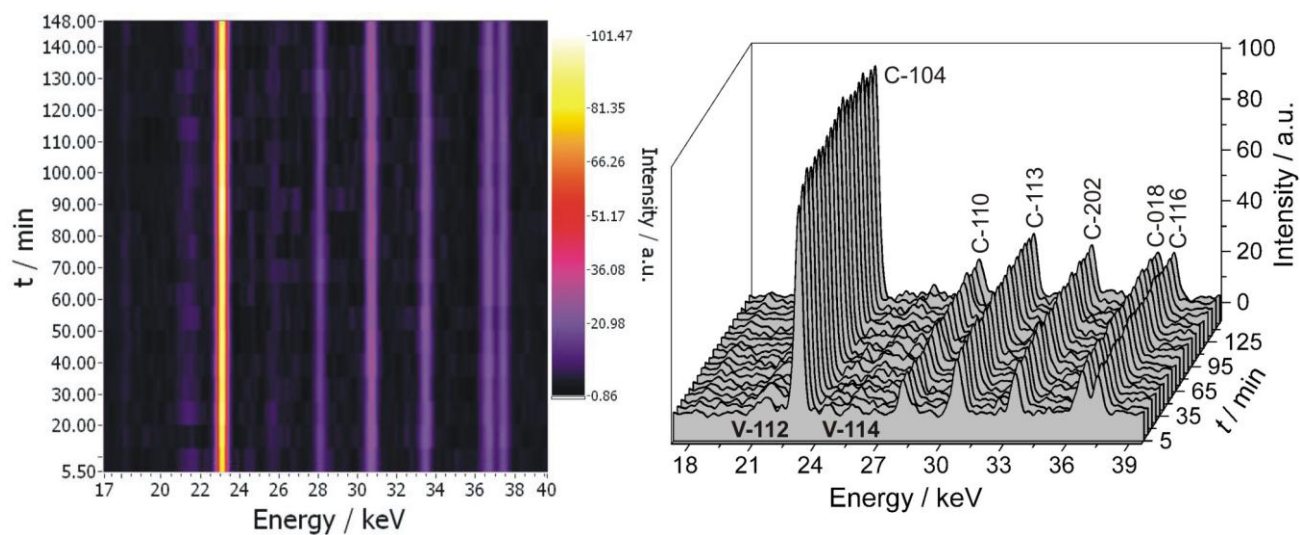
200 ppm SiO₂



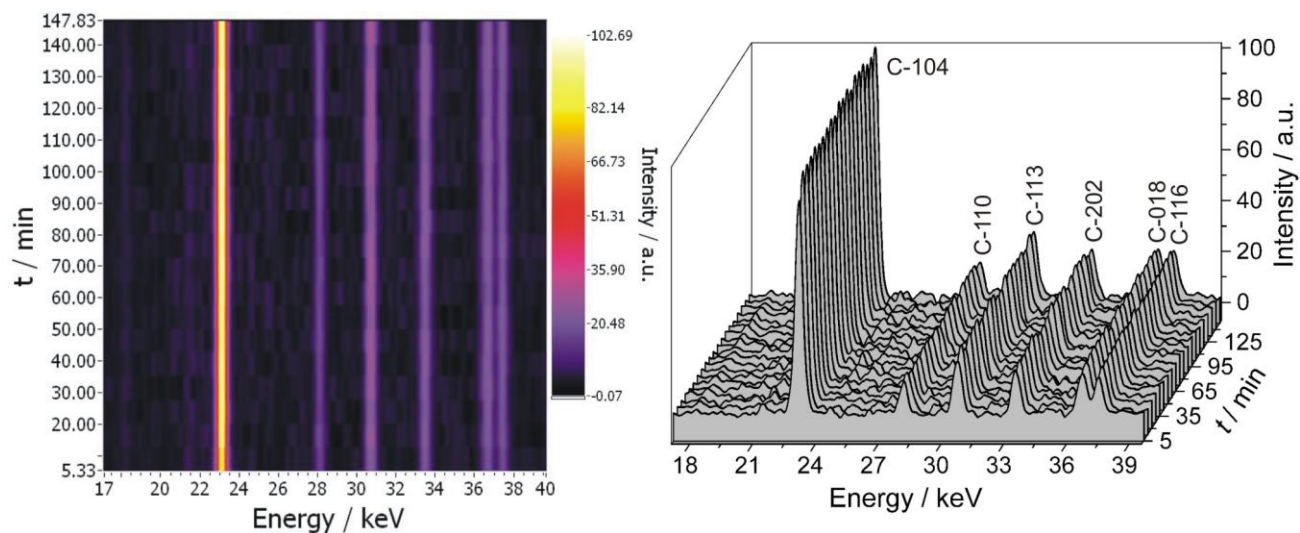
600 ppm SiO₂



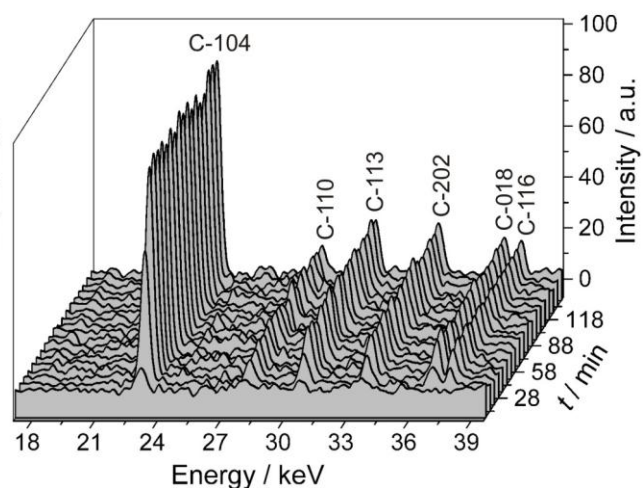
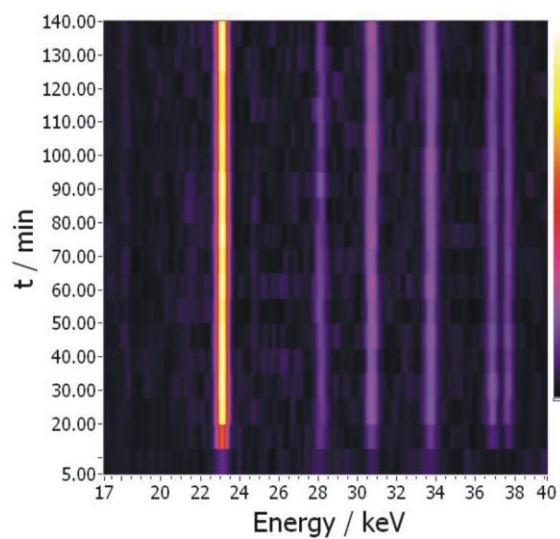
1200 ppm SiO₂



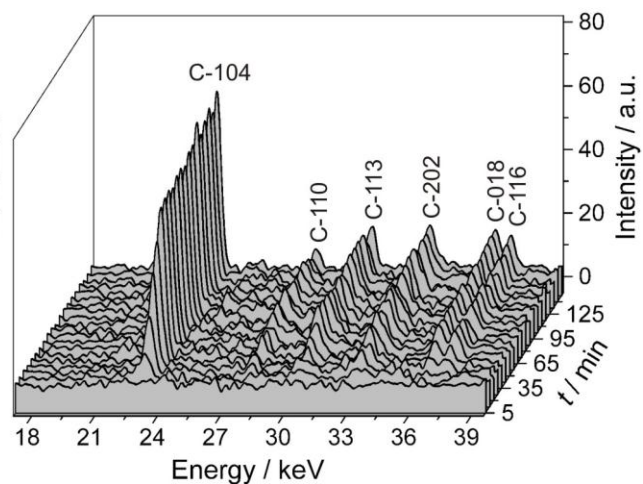
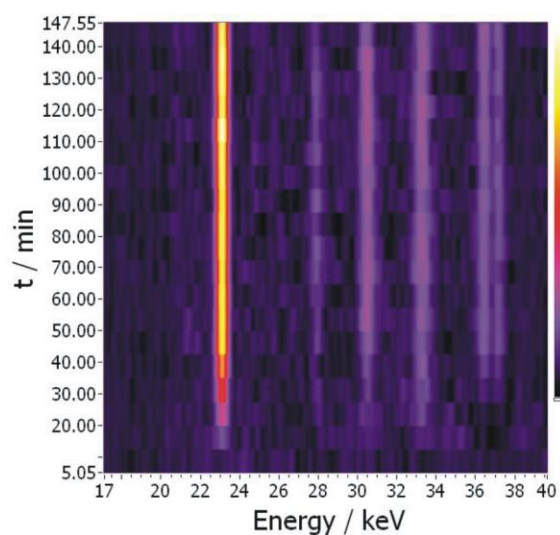
2000 ppm SiO₂



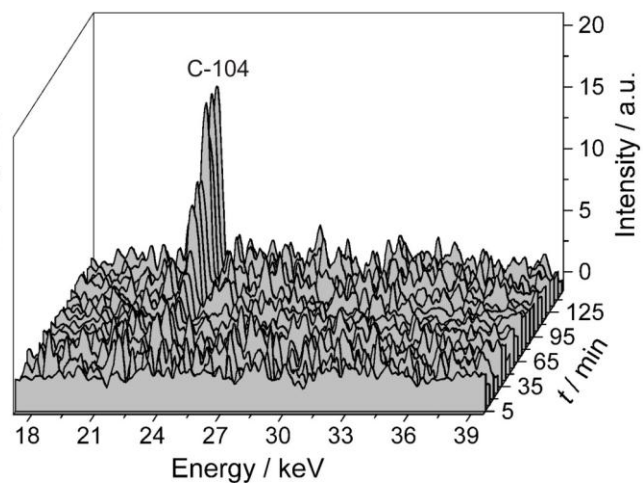
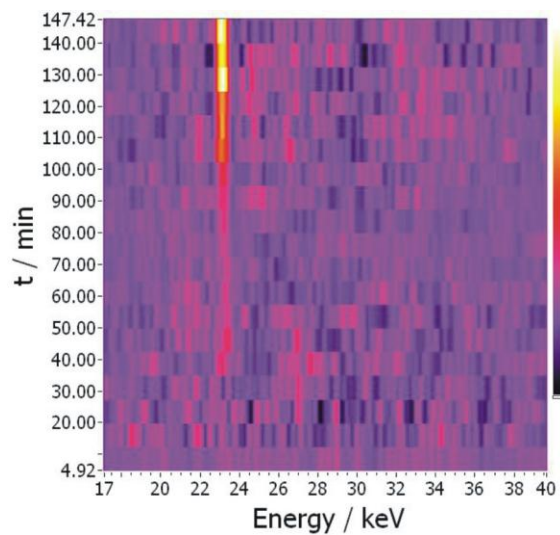
5000 ppm SiO₂



10000 ppm SiO₂

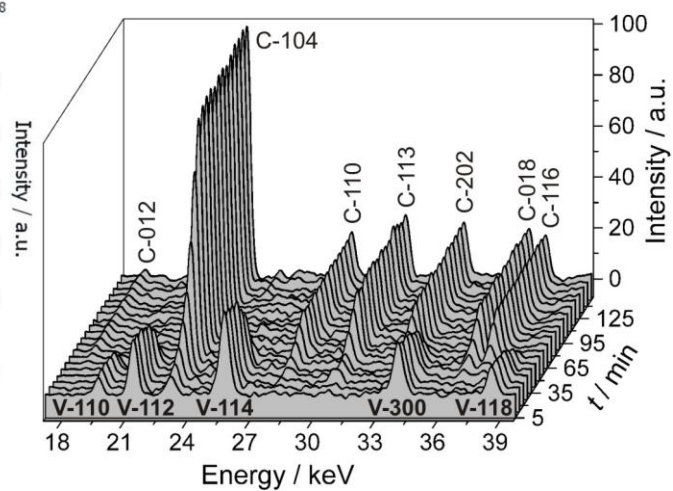
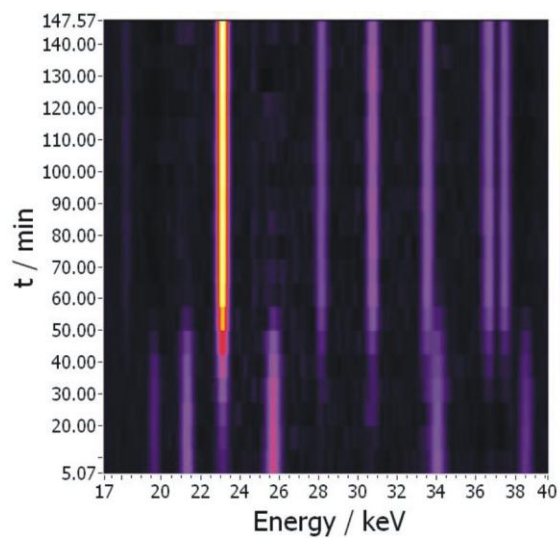


20000 ppm SiO₂

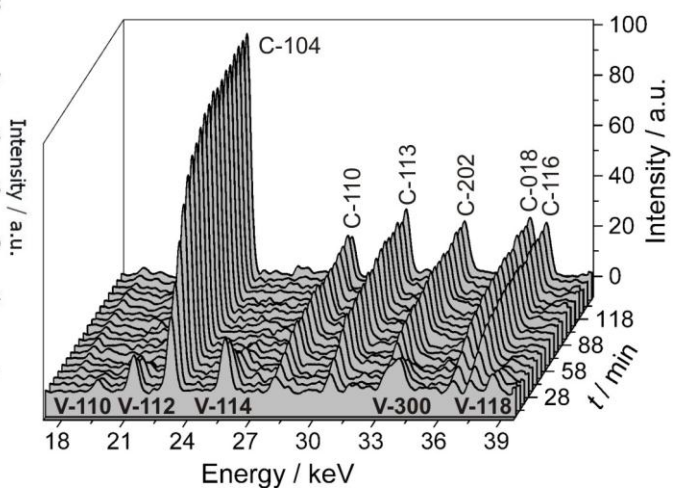
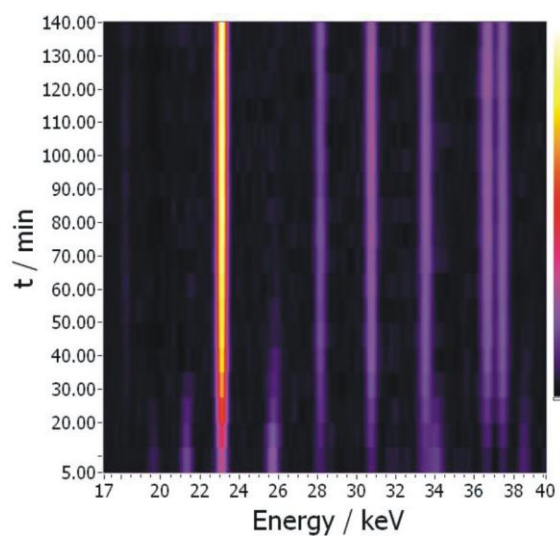


50°C

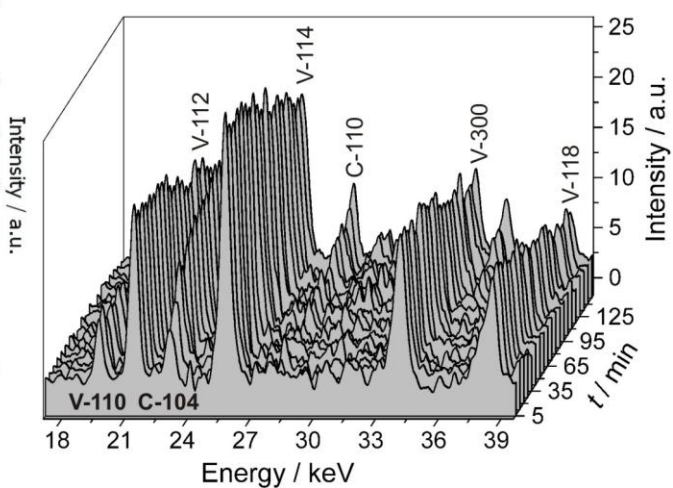
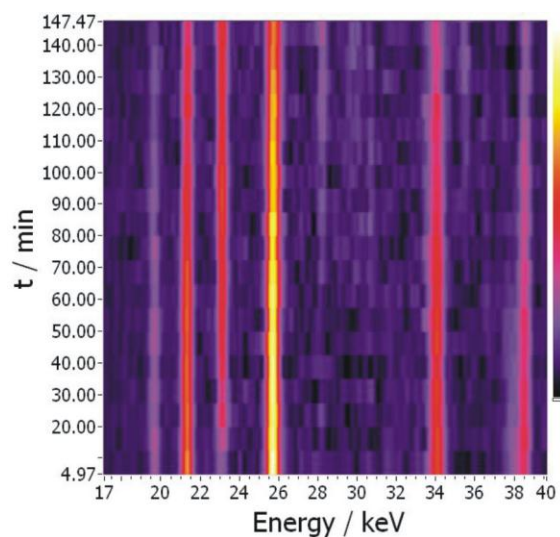
0 ppm SiO₂



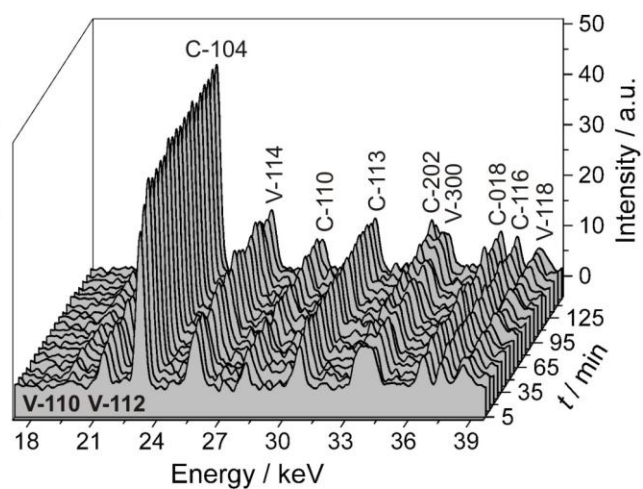
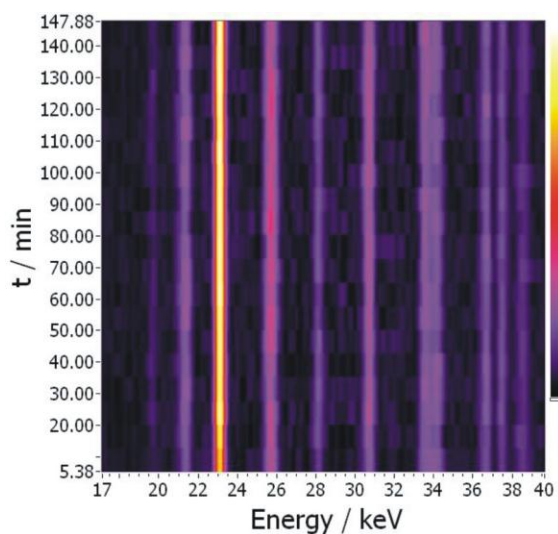
200 ppm SiO₂



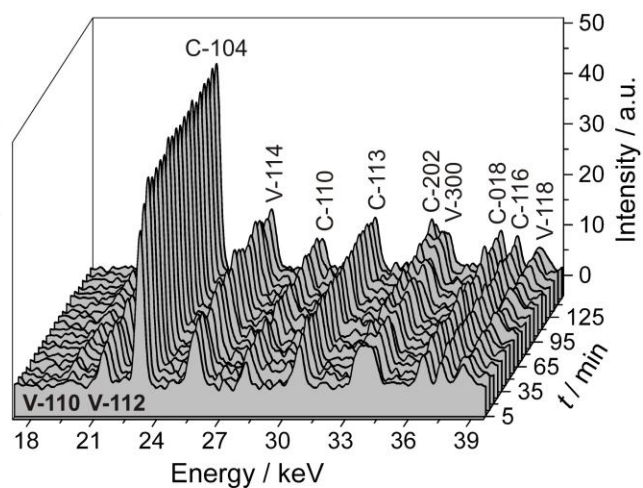
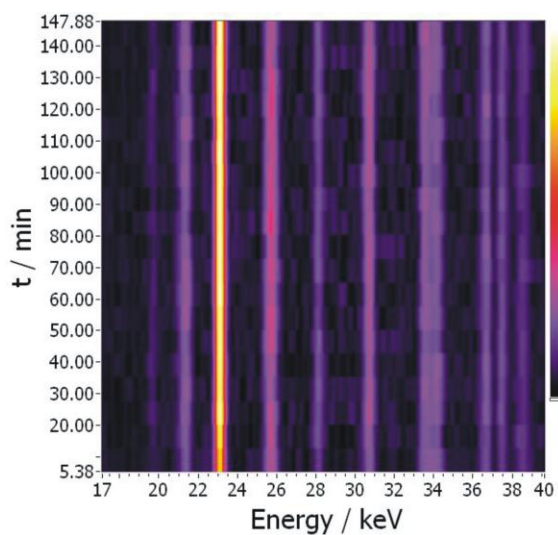
600 ppm SiO₂



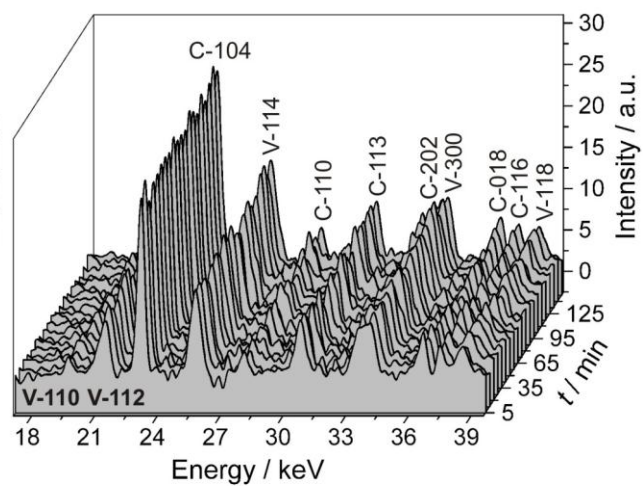
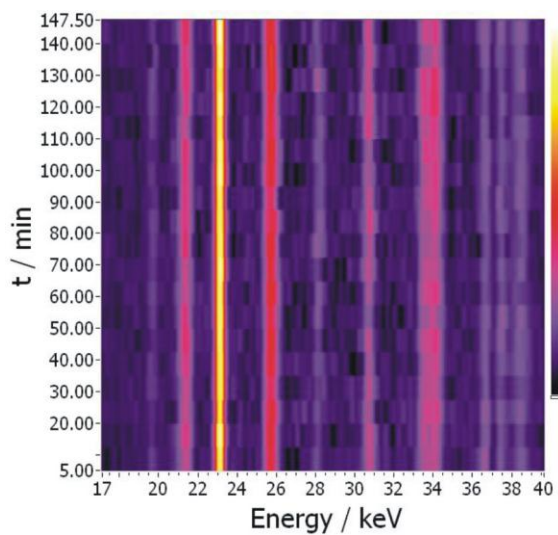
1200 ppm SiO₂



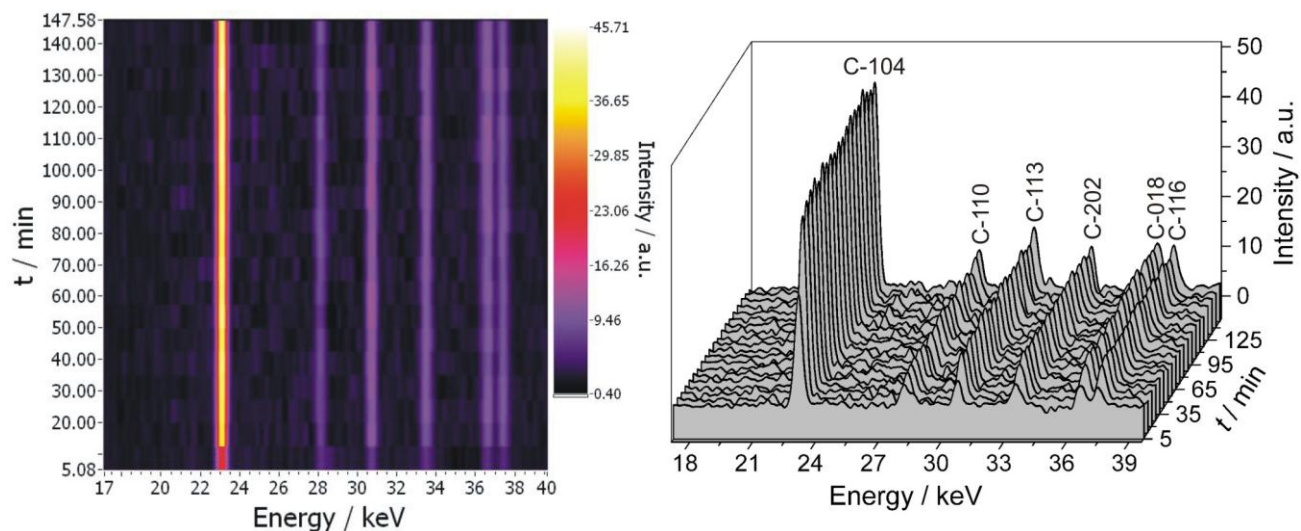
2000 ppm SiO₂



5000 ppm SiO₂

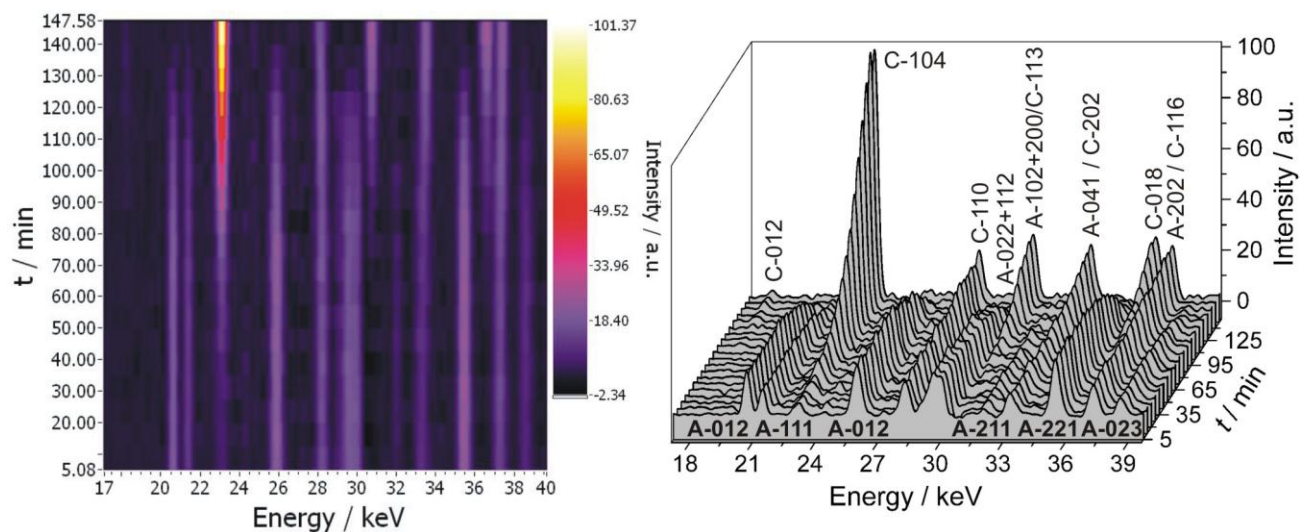


10000 ppm SiO₂

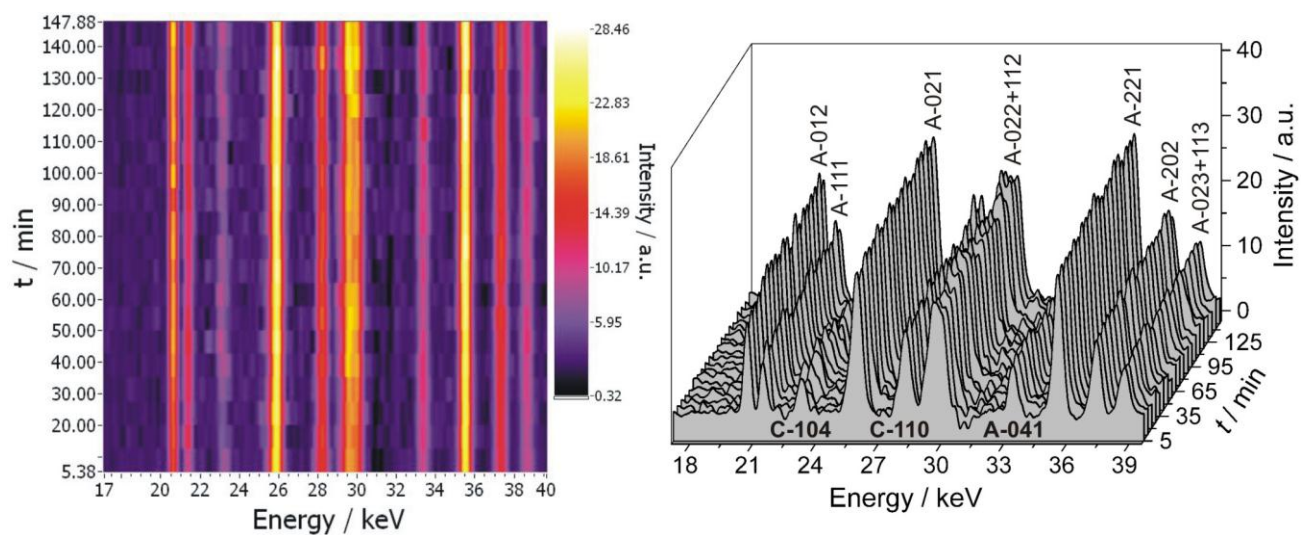


80°C

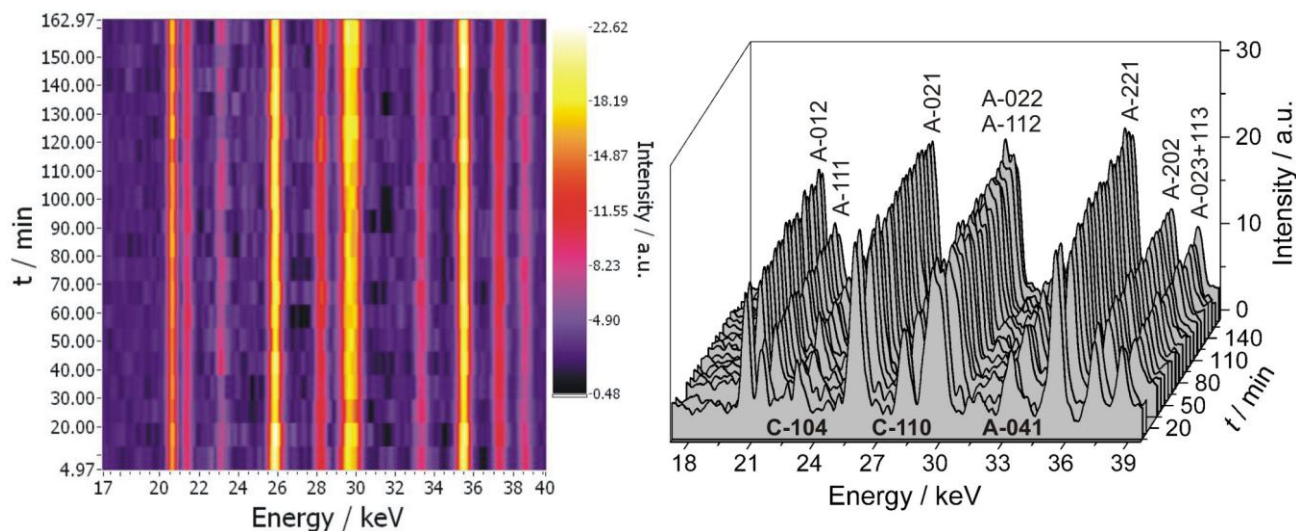
0 ppm SiO₂



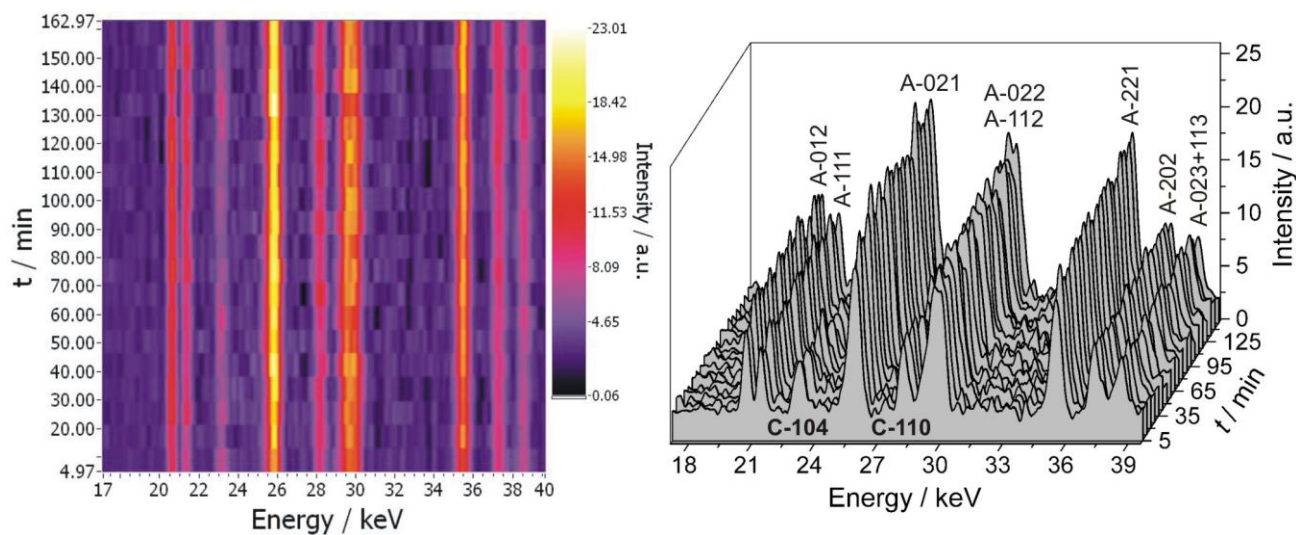
200 ppm SiO₂



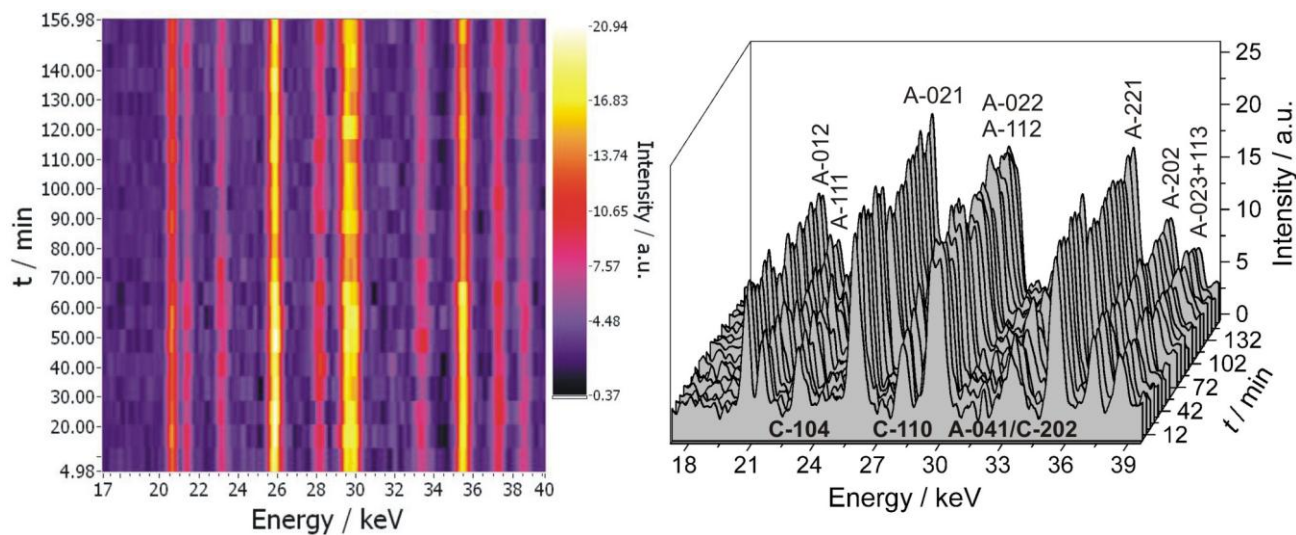
600 ppm SiO₂



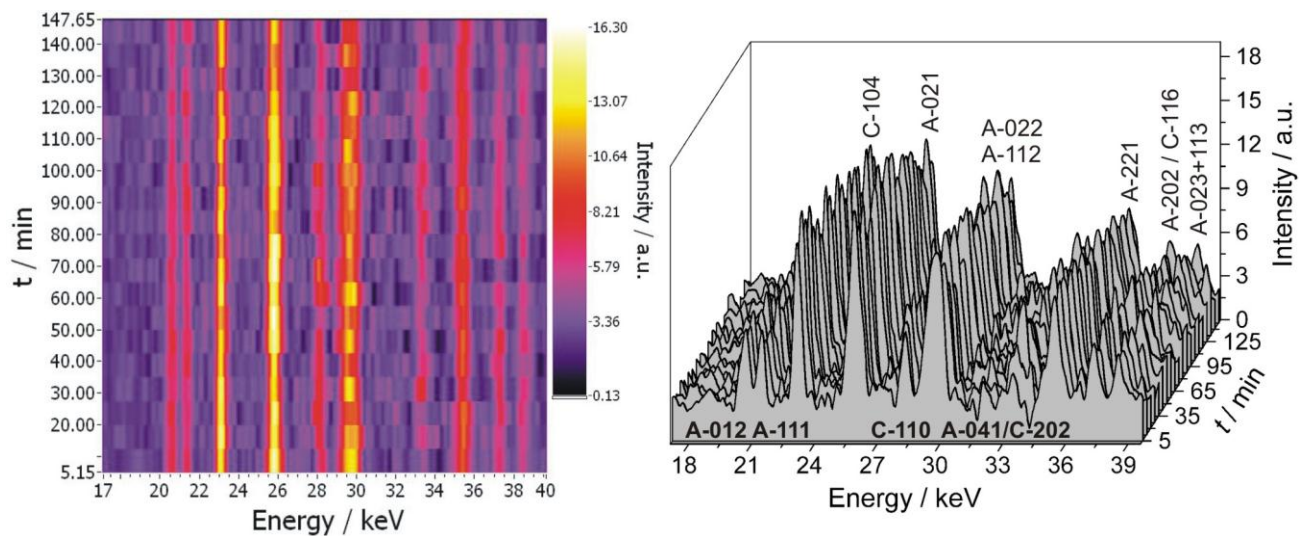
1200 ppm SiO₂



2000 ppm SiO₂



5000 ppm SiO₂



10000 ppm SiO₂

